Journal of Statistical Physics, Vol. 115, Nos. 1/2, April 2004 (© 2004)

Loose, Flat Knots in Collapsed Polymers*

E. Orlandini,[1] A. L. Stella,[1,2] and C. Vanderzande[3,4]

Received April 14, 2003; accepted August 8, 2003

We consider single ring polymers which are confined on a plane but maintain a fixed three-dimensional knotted topology. The equilibrium statistics of such systems is studied on the basis of a model on square lattice in which the configurations are represented by N-step polygons with a number of self-intersections restricted to the minimum compatible with the topology. This allows to define the size, s, of the flat knots and to study their localization properties. Due to the presence of both excluded volume and attractive interactions, the model undergoes a theta transition. Accurate Monte Carlo results show that, while in the high temperature swollen regime both prime and composite knot components are localized ($\langle s \rangle_N \sim N^t$, with $t = 0$), in the low temperature, compact phase they are fully delocalized ($t = 1$). Right at the theta transition weak localization prevails ($t = 0.44 \pm 0.02$). Part of the results can be interpreted by taking into account a dominance of figure eight shapes for the coarse grained knotted polymer configurations, and by applying the scaling theory of polymer networks of fixed topology. In particular $t = 3/7$ can be conjectured as an exact exponent characterizing the weak knot localization at the theta point.

KEY WORDS: Knots; polymers; Monte Carlo.

1. INTRODUCTION

The importance of the presence of knots in long polymer chains can perhaps be best illustrated by referring to the example of DNA.[1,2] In the last decades several experiments have shown the role played by topological entanglement in biological processes involving this macromolecule.[3] Naturally occurring knots in the closed double helix prevent its separation

* Dedicated to Gianni Jona-Lasinio on his 70th birthday.

[1] INFM-Dipartimento di Fisica, Università di Padova, I-35131 Padova, Italy.

[2] Sezione INFN, Università di Padova, I-35131 Padova, Italy; e-mail: attilio.stella@pd.infn.it

[3] Departement WNI, Limburgs Universitair Centrum, Universitaire Campus, 3590 Diepenbeek, Belgium.

[4] Instituut voor Theoretische Fysica, Katholieke Universiteit Leuven, 3001 Heverlee, Belgium.

0022-4715/04/0400-0681/0 © 2004 Plenum Publishing Corporation

into single strands in replication, and impede access to the full genetic code during transcription.[4] Nature therefore introduced enzymes whose function is to systematically change the knot type of circular DNA.[5–7] At the dynamical level, experiments also show that the mobility of circular DNA under electrophoresis depends sensibly on the type of knot.[5, 8–11] These experimental facts concerning DNA largely contributed to turn knotted molecules from a chemical and physical curiosity into one of the hot topics in current polymer conformational statistics and biologically inspired physics. However, this is far from exhausting the motivations of interest for topologically entangled polymers. It has been realized early,[12, 13] and proved rigorously in specific models,[14, 15] that topological entanglement is generated with probability one in the process of polymerization of sufficiently long closed chains.[16] At the same time, many static and dynamic properties of single polymers, or of assemblies of chains, like gels or rubbers, are expected to depend crucially on the ubiquitous self- and mutual topological entanglement at molecular level.[17] Direct probes of the effects of topology are nowadays offered by single molecule manipulation techniques.[18] So, one can anticipate much progress in this field in the near future.

From a theoretical point of view, the statistical or dynamical description of a polymer subject to topological constraints poses challenging difficulties which were recognized since the pioneering works on the subject.[14, 19–23] Topological constraints imply restrictions of the region of configuration space accessible to the system. Being global in nature, these constraints require a full control of the polymer conformation and, except in rare simplified situations,[19] are impossible to implement analytically, e.g. by including suitable terms in a Hamiltonian. In spite of these difficulties, in recent years some progress has been made in understanding the interplay between topology and the critical statistical fluctuations of long polymers.[20, 24–27] Effects of polymer thickness have also been investigated.[28] A consistent part of the progress reported in the above references was achieved through powerful numerical methods (see, in particular, refs. 20, 24, and 25). An obvious question is whether the scaling laws valid for a closed polymer without constraints, remain unaltered when only a specific topology is allowed. This seems to be the case for the scaling law relating the average radius of gyration to the total chain length. For polymers in good solvent, the ν exponent of this law does not appear to be affected by the restriction to a fixed knot type.[30–32] This and other numerical results indicate that knots are statistically rather tight and involve relatively small fractions of the total chain length. This localization was first conjectured by comparing the rate of growth with length of the number of possible configurations of a knotted ring to that valid for an unknotted

one.[33] The ratio of the growth rates is a power of the chain length which can be simply interpreted in terms of the multiplicity of positions that a tight knot can assume along the chain itself.

An important step towards a more precise quantification of what "tight" precisely means for knots, and in the description of how the narrow localization combines with the global scale invariance, was made most recently through the study of "flat knots." These knots, which were introduced in ref. 39, could in principle be concretely realized by adsorbing an entangled ring polymer on an attractive planar surface,[34] or by confining it between two close parallel walls. Macroscopic realizations of flat knotted polymers were also considered in experiments on vibrated granular necklaces.[35] These systems are definitely, though only slightly, out of equilibrium,[36] unlike those considered in the present paper. Polymers with flat knots are especially amenable to a topological study, because they constitute a concrete realization of those projections onto a plane on which knot theory bases the definition and evaluation of topological invariants.[37] If the number of overlaps of the polymer on itself is restricted to the minimum compatible with the topology, the study of flat knots enjoys some drastic simplifications with respect to the harder problem of three-dimensional knots. The overlaps of the chain can be interpreted as vertices of a two-dimensional polymer network, for which a well developed theory exists, especially in two dimensions.[40, 41] At the same time the results for such flat knots should give qualitative indications about the properties of real knots in three dimensions. By exploiting results of polymer network theory in two dimensions and numerical simulations, Metzler *et al.*[39] were able to show that prime flat knots in a self-avoiding chain are strongly localized, in the sense that their average size, s, which can be unambiguously defined, does not grow as a positive power of the total chain length. They could also show that the probability distribution function for the knot sizes asymptotically is a power law consistent with this non-diverging first moment. Interestingly enough, the scaling analysis of ref. 39 was inspired by a recent approach to DNA denaturation, which was also based on polymer networks.[42]

The above results on the localization of regular and flat knots leave open interesting, further issues. An obvious one is of course the possible extension of the study to knots in three dimensions.[43, 44] In the present paper we concentrate on a similarly ambitious problem. We want to understand the effects of attractive interactions inducing polymer theta collapse[45] on the localization of flat knots. There are several motivations to be interested in such an issue. Besides the validity per se as a frontier problem in lattice statistics, such a study at the moment seems to be the only realistic way to get indications on the behavior of knotted polymers

undergoing collapse in three dimensions. In spite of the central role played by theta collapse in the conformational statistics of macromolecules, to our knowledge, until now there are neither experimental nor theoretical results available on the localization properties of knots in polymers undergoing such transition. On the other hand, it has been pointed out recently that several proteins in their native state can be considered as knotted, even if they are open chains.[46, 47] This raises immediately interest in the possible interplay between collapse and knot localization. Indeed, one of the accepted scenarios for protein folding implies that the native state is reached after the protein enters in a compact molten phase.[48] In the case of a knotted protein, it then becomes crucial to have an idea of whether in the molten phase the knot is localized or not. On the basis of this alternative, one can anticipate completely different features for the dynamical process by which the protein can eventually reach its native conformation. As we will show below, the condition of being compact for a polymer can involve a novel behavior in relation to the localization of possible knots. In contrast to the localization systematically encountered so far for polymers in swollen regimes,[39] or under the effect of repulsive interactions,[49] a flat knot in a collapsed polymer turns out to be delocalized. This means that the flat knot statistically tends to occupy the whole chain, rather than a small fraction of it, even if the chain becomes infinitely long.

As far as we can see, flat knots of polymers below the theta transition constitute the first example of delocalized topological entanglement reported so far. The present paper presents a numerical and theoretical study which allows to show that the theta collapse of self-attracting flat polymers marks a localization-delocalization transition for the knots. Our approach is based heavily on numerical simulation. At the same time, we are able to interpret some of our findings in the light of results of the theory of polymer networks in two dimensions.[40] The connection we can establish here with polymer networks shows analogies between our problem and some features emerging in recent studies of the denaturation transition of DNA.[42] Indeed, in that context the application of polymer network pictures revealed also quite successfull and led, among other things, to the conclusion that denaturation can be to a large extent understood and represented in terms of a simplified structural motiv (a single denaturated loop from which two long double stranded segments depart) which somehow dominates the conformational statistics.[42, 50] A similar dominance seems to occur for various flat knots in several conditions, the motiv being in this case the two-loop, number eight conformation. In both contexts the existence of a dominating conformational motiv is an important aspect of the physics which considerably simplifies the interpretation of some results.

The present paper is organized as follows. In the second section we present the lattice model that we used for our numerical work, introduce the problem of flat knot localization and describe our Monte Carlo strategy. In the third section we discuss a simple, prime flat knot (3_1) at different temperatures, showing that it undergoes a localization-delocalization transition at the theta point. The behavior at the theta point is further analysed in Section 4, where we illustrate how a polymer network picture can be used to interpret some of the observed scalings. In Section 5 we analyse the behavior of more complex knots, including those that are composite. The last section is devoted to conclusions.

A short report containing part of our results was published earlier.[51]

2. POLYMER RINGS WITH FLAT KNOTS

The model[38] we study is defined on the square lattice. A configuration of a ring polymer in good solvent is represented by a self-avoiding polygon (SAP), i.e., a closed lattice walk whose steps can visit each edge and each vertex of the lattice at most once. In order to introduce the possibility of topological entanglement, we further allow the polygon bonds to be on the diagonals of elementary lattice plaquettes. When such an option is taken, both diagonals of the elementary square must be simultaneously occupied by bonds and one needs to further specify which of the two bonds lies over the other. In this way each one of these intersections assumes the meaning of overlap of the polymer with itself and the model can describe the topological entanglement appropriate for a three dimensional knotted ring constrained to lie on a plane. Of course, even if this ring is unknotted, there can still be self-intersections in its two dimensional conformations. The difference between a knotted and an unknotted ring is reflected by the fact that only for the latter, one can eliminate all the intersections by a set of continuous deformations, such as the lattice implementations of the Reidemeister moves introduced in ref. 38. If there is a knot in the ring, its flat realization will always show at least a minimum number of intersections, which coincides with the crossing number as defined in knot theory.[37] In Fig. 1 we show the configuration of a flat trefoil knot (3_1) according to our model.

The excluded volume restrictions and crossing conditions specified above are such to determine for this model a SAP scaling behavior if all allowed configurations are weighted equally. Indeed, even if the number of overlaps is completely unrestricted the canonically averaged square radius of gyration, $\langle \vec{R}_g^2 \rangle_N$,[5] has been shown in ref. 38 to grow with the number of

[5] Here $\langle . \rangle_N$ denotes a canonical average of polygons with N steps.

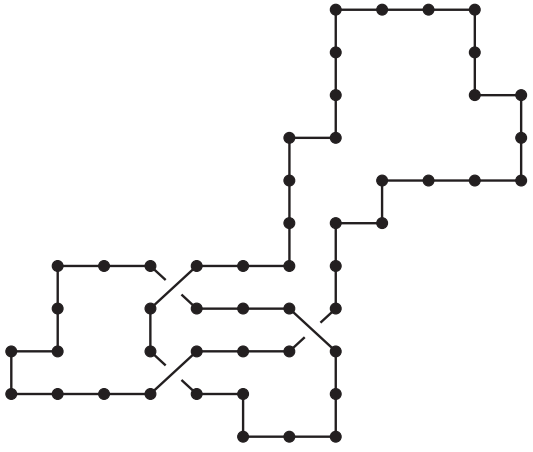

Fig. 1. A ring polygon with the topology of the trefoil knot and with a minimal number of self-intersections.

polygon edges, N, as $\langle \vec{R}_g^2 \rangle_N \sim N^{2\nu}$, where ν is consistent with the value 3/4 appropriate to SAP in two dimensions.[52] For each configuration one defines $\vec{R}_g^2 = \sum_i (\vec{R}_i - \vec{R}_{cm})^2/N$, where $\vec{R}_i$ are the positions of the vertices of the polygon, and $\vec{R}_{cm}$ is their center of mass. The model can be further specified by introducing an interaction controlling the number of intersections: each crossing is assumed to involve an increase in energy $E > 0$, so that a configuration with N_c crossings contributes a Boltzmann weight $w^{N_c} = \exp(-EN_c/T)$, where T is the absolute temperature. Thinking to an adsorbed polymer, E can be interpreted as the opposite of an adsorption energy to be payed in order to create a crossing. Low values of w will reduce $\langle N_c \rangle_N$, but never below its minimum. In fact our results below are obtained for w very close to zero, so that N_c allmost always stays at its minimum. In order to allow the possibility of theta collapse, we introduce in our model an attractive interaction potential which lowers the total energy by $\varepsilon > 0$ whenever two nearest neighbor lattice sites are visited by nonconsecutive vertices of the polygon. As discussed below, this attractive interaction is sufficient to induce a theta collapse at sufficiently low temperature T. The Hamiltonian of a polygon configuration ω with $N_c(\omega)$ crossings and $N_i(\omega)$ nearest neighbor interactions is $H(\omega) = EN_c(\omega) - \varepsilon N_i(\omega)$. Below we will always choose units such that $\varepsilon = 1$ and will omit to specify dependences on E/T. Indeed, E/T is always kept very large and the corresponding small and rare fluctuations of N_c above its minimum are only allowed in order to improve the mobility of our Markov chain in configuration space.[38] [6]

[6] A rigorous proof of ergodicity does not exists for our algorithm. However, in ref. 38 arguments in support of ergodicity were produced.

While very intuitive, the concept of length of a knot in three dimensions poses the problem of a meaningful operative definition.[43] This is not the case for flat knots in our model, when they are observed in polymer configurations with the minimum number of crossings. These configurations in the case of a flat trefoil (3_1) for example are such that the whole chain backbone is partitioned into six arcs, each of which is incident on two of the three overlap points. We can denote the lengths of these six arcs by $l_1, l_2, \ldots, l_6$, with the understanding that the numbering is in order of increasing length, i.e., $l_1 \leqslant l_2 \leqslant \cdots \leqslant l_6$. Clearly, if the total length of the ring N grows to infinity, at least $\langle l_6 \rangle_N$ must grow like N, since $N = \sum_i \langle l_i \rangle_N$. The length of the knot, l, can then be assumed to be given by $s = N - l_6$ and the behavior of $\langle l_5 \rangle_N$ for large N can be used in order to definine the degree of localization. For example, if $\langle s \rangle_N \sim \langle l_5 \rangle_N \sim N^t$, with $0 \leqslant t < 1$ we talk about a localized knot. If $\langle s \rangle_N \sim \langle l_5 \rangle_N \sim N$ the flat knot is delocalized, since the entanglement extends on average to the whole ring.

We studied the model by a Monte Carlo approach which induces a Markov process in the space of configurations ω. The transitions between different configurations are determined by combinations of local and nonlocal moves which are such to leave the topology invariant, i.e., do not modify the type of knot. These moves are described in ref. 38. The statistical ensembles considered are grand canonical with a fugacity K assigned to each polygon step. At a given temperature T a multiple Markov chain (MMC) approach is used in which configurations are exchanged among ensembles at different step fugacities K. This is done in order to improve the efficiency of the sampling especially at low T.[53, 54] Our multiple chains combined up to 10 processes at different K's.

3. NUMERICAL RESULTS FOR THE TREFOIL

We start by discussing the trefoil, the simplest example of a prime flat knot. We first determined $\langle \vec{R}_g^2 \rangle_N$ by selecting from a grand canononical simulation those polygons ω whose total number of steps falls into a narrow window centered at a particular N value. In order to enrich the sampling at large N the maximal fugacity in the set defining our MMC's had to be always chosen very close to the critical value $K_c(T)$ above which $\langle N \rangle = \infty$ in the grand-canonical ensemble. Log-log plots of $\langle \vec{R}_g^2 \rangle_N$ in a wide range of N showed that while at high temperature $\nu \sim 3/4$, as appropriate for a swollen ring, for low temperature $\nu \sim 1/2$, indicating that the polygons become compact. A precise localization of the theta transition was made by identifying T_Θ with the T value for which our plots showed the best agreement with the expected theta point exponent $\nu = 4/7$.[55] In this way we got $T_\Theta = 1.49 \pm 0.05$ which is remarkably close to the value

(1.4988 ± .0007) appropriate for rings without any self crossings.[56, 57] The existence of a theta point, and the essential coincidence of T_θ with the theta temperature of SAP's could be expected especially in view of the fact that, as discussed below, in the high T and theta regimes the flat knot appears to be localized.

For large N, $\langle l_5 \rangle_N$ was found to have different behaviors above, at and below T_θ (see Fig. 2). For $T > T_\theta$ this average was found to approach a constant asymptotically, consistent with $t = 0$. For $T = T_\theta$, $\langle l_5 \rangle_N$ increases as a power of N and we determined $t = 0.44 \pm 0.02$.[51] So, at the theta point the localization becomes weaker than at high T and is described by a t exponent which we will try to interpret in the next section. MC runs at $T = 1.2 < T_\theta$ showed a remarkable and somehow unexpected behavior of $\langle l_5 \rangle_N$. While at relatively low N this quantity appeared to follow a power law with t slightly larger than the theta point value, for $2000 \lesssim N \lesssim 3000$ its growth turned definitely linear in N. Thus, $t = 1$ qualifies as the most plausible asymptotic exponent. This conclusion is supported by the circumstance that the statistical error bars for $\langle l_5 \rangle_N$ do not exceed 12% in the region $\ln N \geqslant 6$. To our knowledge, this last result[51] is the first example of knot in a delocalized state met so far.

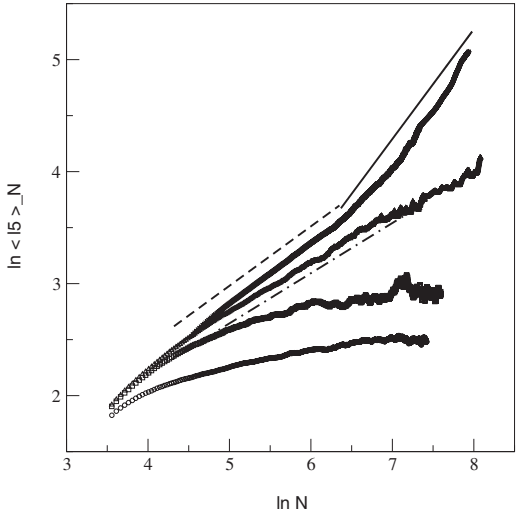

Fig. 2. Log-log plot of $\langle l_5 \rangle_N$ as a function of N for a trefoil knotted polymer. From bottom to top: $T = \infty$, 2.0, 1.49, and 1.25. The slopes of the straight lines are: 0.44 (dot-dashed), 0.66 (dashed), and 1 (full).

4. POLYMER NETWORKS AND THE DOMINANCE OF FIGURE EIGHT CONFIGURATIONS

If one interprets the intersection points as 4-leg vertices and if all l_i's are $\gg 1$, the configurations of the flat trefoil can be regarded as those of a polymer network with six macroscopic segments in two dimensions. The theory of such networks has been developed by Duplantier,[40] Schäfer *et al.*,[58] and Ohno and Binder.[41] In ref. 42 the results of such theory were successfully applied in order to predict the scaling of the probability distribution function of denaturated loops of DNA at melting. Inspired by these progresses, Metzler *et al.*[39] used similar arguments to discuss the scaling of the length distribution of prime flat knots in good solvent conditions. Along similar lines we apply here network theory in the case of polymer networks with both excluded volume and attractive interactions, as required by our model.

A polymer network of given topology G is specified by the number of vertices of degree k, n_k ($k = 1, 2, 3,\ldots$), and by the lengths, $l_1, l_2, l_3,\ldots, l_m$, of the m segments joining the vertices. Keeping the various l_i's of the order of $N = \sum_i l_i$, the total network length, the partition function can be put in a form[40, 58]

$$Z_G(l_1, l_2,\ldots, l_m) = K_c^{-N} l_m^{\gamma_G - 1} F_G(l_1/l_m, l_2/l_m,\ldots, l_{m-1}/l_m) \tag{1}$$

where F_G is a scaling function and

$$\gamma_G = 1 - \nu\, dL + \sum_k n_k \sigma_k \tag{2}$$

In the last equation d is the dimension of the embedding space (2 in our case) and L is the number of independent loops in the network. Figure 3 gives an example of network with $m = 7$, $n_1 = 2$, $n_4 = n_3 = n_5 = 1$, $L = 3$. The exponent γ_G and the function F_G convey the dependence on the specific topology of the network. The exponent σ_k is an anomalous scaling dimensions associated to each k-leg vertex and in some cases it can be calculated by field theoretical renormalization group methods in ϵ-expansion for models describing the polymer in the continuum.[40] In two dimensions, Coulomb gas techniques have allowed exact predictions of σ_k, for both good solvent ($T = \infty$),[40] and theta conditions.[55] Since Eqs. (1) and (2) assume the polymer segments to be macroscopic, application to the case of the network corresponding to the flat trefoil knot requires that all six segments are much longer than a single lattice step. For configurations of the knotted polymer in which some of the segments remain microscopic ($l_i \sim 1$), Eqs. (1) and (2) are expected to hold for an effective, contracted

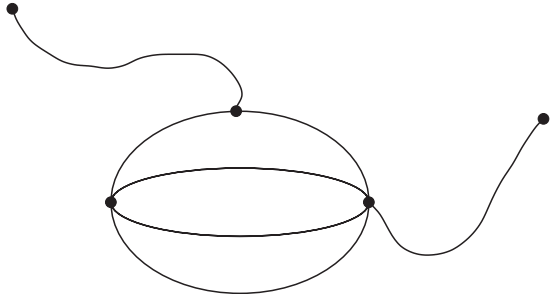

Fig. 3. A polymer network with $m = 7$, $n_1 = 2$, $n_4 = 1$, $n_3 = 1$, $n_5 = 1$, and $L = 3$.

network with fewer segments and, possibly, fewer and modified vertices. A careful statistical analysis of the configurations obtained in our runs for the trefoil knot at both $T > T_\theta$ and $T = T_\theta$ show that indeed a contracted network description applies to these cases. Consider for example the case $T = T_\theta$. The configurations sampled in our simulation show that while l_5 fluctuates rather broadly, within a range growing with N, the same does not apply to l_4, which takes most often microscopic values ($l_4 \sim 1$) and fluctuates much less. It is then natural to assume that the dominant configurations of the trefoil are represented by a contracted network, with only two segments and a four-leg vertex: this is a figure eight. By applying Eqs. (1) and (2) and by assuming consistently with the numerics that $l_5 \ll N$, one can then derive the behavior of $p(l_5)$ the probability distribution of the values taken by l_5. Indeed, for a figure eight network with segments of length $N - l_5$ and l_5 the partition function should scale as

$$Z_8(N - l_5, l_5) \sim K_c^{-N} (N - l_5)^{\gamma_8 - 1} F_8\left(\frac{l_5}{N - l_5}\right) \tag{3}$$

Here $\gamma_8 = 1 - 2dv + \sigma_4$, where $v = 4/7$ at the theta point.[55] On the other hand, the values of σ_k are exactly known for a network at the theta point. Since the system is described by the critical low-T phase of the $O(n = 1)$ n-component spin model, Coulomb gas methods allow to derive $\sigma_k = (2 - k)(2k + 1)/42$.[55] This implies $\gamma_8 = -12/7$. Now, for $l_5/N \to 0$, the partition function in Eq. (3) should reduce to that appropriate for a self-avoiding ring of N steps at the theta point, which scales as

$$Z_o(N) \sim K_c^{-N} N^{-dv}, \tag{4}$$

again according to Eq. (1). Since Eq. (3) must match Eq. (4) in the limit $l_5/N \to 0$, we conclude that the scaling function F_8 for small x should scale

as $F_8(x) \sim x^{-c}$, with c chosen in such a way that the l_5 dependence in Eq. (3) disappears. This implies $c = 1 - \gamma_8 + dv = 11/7 = 1.57$. Hence, for $l_5/N \ll 1$,

$$Z_8(N - l_5, l_5) \sim K_c^{-N} (N - l_5)^{-dv} l_5^{-11/7} \tag{5}$$

and this clearly also implies $p(l_5) \sim l_5^{-c} = l_5^{-11/7}$. From the last equation we get immediately that $\langle l_5 \rangle \sim N^{3/7}$. This result is consistent with the numerical estimate $t = 0.44 \pm 0.02$ we made on the basis of our MC data. Such consistency shows that at the theta point the configurations of the flat trefoil are dominated by the figure eight motiv. A similar dominance of the figure eight holds in fact also at $T > T_\theta$. This was already argued in ref. 39 in the $T = \infty$ case by studying the probability distribution $p(l_5)$ obtained from MC simulations of an off-lattice model of a flat trefoil knotted chain. This distribution was found consistent with the value of c that can be deduced along the same lines as above but using as inputs the σ_4 and the ν appropriate to a polymer in good solvent. In this case $\nu = 3/4$,[52] and $\sigma_k = (2-k)(9k+2)/64$ follows again by Coulomb gas methods applied to a critical $O(n = 0)$ model.[40] The value of c obtained in the $T = \infty$ case is $43/16 > 2$, consistent with the fact that the first moment of $p(l_5)$ does not diverge for $N \to \infty$, i.e., with $t = 0$ (See also Fig. 2). Indeed, since the natural cut-off for the power law behavior $p(l_5) \sim l_5^{-c}$ is N, only for $c \leqslant 1$ one expects a divergent first moment. We verified numerically, by simulations at $T = 2.0 > T_\theta$ that the behavior valid for $p(l_5)$ at $T = \infty$ holds also at finite temperature above the theta point. This confirms the expectation that the whole region $T > T_\theta$ can be considered as a unique phase as far as the localization regime of the knot is concerned.

An obvious question is now whether one could hope to get similar insight into the delocalization we got at $T < T_\theta$. In the argument presented above for the theta point a crucial assumption is that one can consider $l_5 \ll N$. If this is not the case Eqs. (1) and (2) can not tell much about the degree of localization. The fact that $\langle l_5 \rangle_N \sim N$ for large N implies that such assumption is not legitimate. So, the delocalization result, certainly the most relevant described above, rests completely on numerical evidence at the present stage. Network scaling theory can however help in a tentative interpretation of the rather extended preasymptotic regime revealed by the plot in Fig. 2 . For an initial interval of about three decades the plot at $T < T_\theta$ shows a slope ~ 0.66, which would be consistent with a weak localization rather than with delocalization.

There are results for polymer network theory which could correspond to the situation of a collapsed polymer below the theta point. One plausible candidate to represent such a polymer is the so called dense polymer.[59]

For such a system Eq. (1) would hold in a modified form including an extra factor growing as an exponential of $N^{1/2}$. This factor takes into account entropy effects due to the presence of a sharp interface for the dense polymer. Apart from this detail, the σ_k of dense polymers in $d = 2$ are known on the basis of the connection with the low-T phase of the $O(n = 0)$ model and one has $\sigma_k = (4-k)^2/32$.[59] Under the assumption that also in the preasymptotic low T regime the statistics is dominated by figure 8 configurations, the arguments presented above for the $T = T_\theta$ case can be repeated giving $c = 11/8$ or $t = 5/8$, nicely consistent with the effective exponent $t = 0.66 \pm 0.07$ observed numerically.

This last argument, together with the other results of this section, shows that the dominance of figure eight configurations is a rather general feature in the conformational statistics of the flat trefoil knotted polymer. At the theta point this dominance could well hold also in a strict asymptotic sense. On the other hand, below the theta transition it is certainly only a transient effect, determined by the fact that the total length of the polymer needs to exceed a certain threshold before delocalization fully prevails. As discussed also below, such threshold effects seems to be rather spread in the statistics of topologically entangled polymers. In principle one can not totally exclude that even at $T = T_\theta$ the dominance of figure eight configurations could amount to a preasymptotic effect. However, to answer this doubt would require to go far beyond the limits of our present computational power.

5. OTHER FLAT KNOTS AND COMPOSITE KNOTS

An obvious question raised by the results for rings with the 3_1 topology is whether the whole scenario of the delocalization transition generalizes to the case of more complex prime knots, or to knots resulting from the composition of two or more prime elements.

Let us consider first more entangled prime flat knots. We studied in particular polymers with a 5_1 or a 7_1 knot.[37, 38] The first issue is whether these knots undergo a delocalization transition of the same type as 3_1. In Fig. 4 we report log-log plots of the average of the second longest arc length for ring polymers with flat knots of type 3_1, 5_1, and 7_1 at $T = 1.2 < T_\theta$. It appears clear that, even if the preasymptotic regimes last somewhat longer for the more complex knots, in all the three cases the curves tend to the same slope ~ 1 for N sufficiently large. This means that the delocalization takes place in all cases.

It is also interesting to verify whether the dominance of figure eight configurations, which played such an important role for $T \geqslant T_\theta$ in the 3_1 case, holds more generally. Figure 5 shows log-log plots of $\langle l_5 \rangle_N$, $\langle l_9 \rangle_N$,

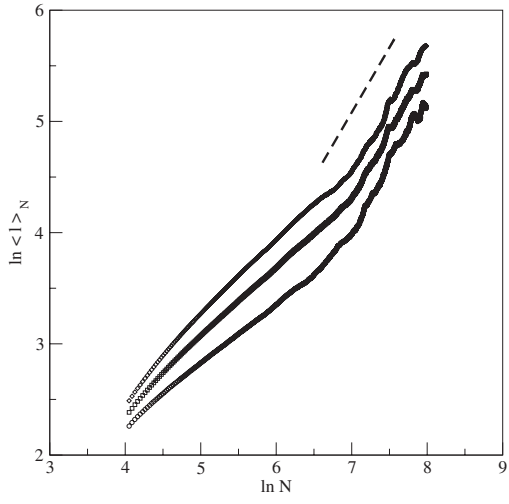

Fig. 4. Log-log plot of the average length of the second largest arc as a function of N for rings with the topology of the 3_1, 5_1, and 7_1 knot (bottom to top). The dashed line has slope 1. The results are for $T = 1.2 < T_\theta$.

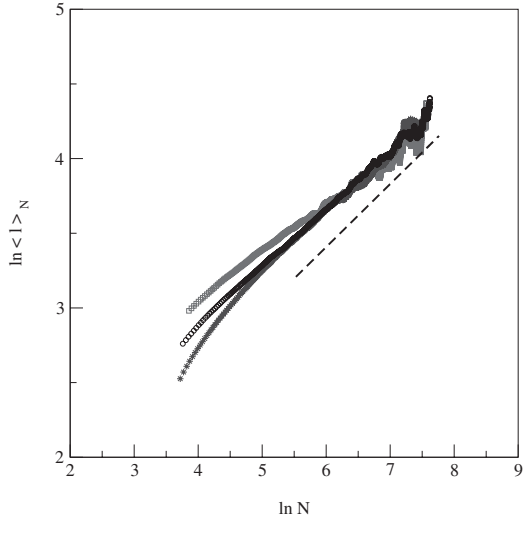

Fig. 5. Log-log plot of the average length of the second largest arc as a function of N for rings with the topology of the 3_1, 5_1, and 7_1 knot (top to bottom). The results are for $T = T_\theta$. The dashed line has slope 0.44.

and $\langle l_{13} \rangle_N$, for the knots 3_1, 5_1, and 7_1, respectively. The temperature is T_θ. In the diagram the three curves are vertically translated in such a way to obtain an overlap among their most asymptotic portions. The good overlap indicates that at the theta point the second longest segment of all three knotted rings grows with approximately the same power of N. In view of the discussion of the previous section, this further suggests that also for 5_1 and 7_1 the dominant configurations can be assimilated to the figure eight. The more complicated microscopic structures underlying the effective 4-leg vertex of the figure eight for the 5_1 and 7_1 cases do not seem to require any modification of the exponent σ_4 to be associated to it.

The behavior of composite knots[37] is also intriguing. We considered the simplest case, $3_1\#3_1$ (# is the standard notation for the sum of knots). The composite character of this knot raises immediately the question of how each component influences the other. In addition, one would like to check whether the figure eight configuration still plays a special role in this case. In this respect we found particularly instructive the study at $T = T_\theta$. Our simulation results show that after an initial transient, the two longest segments of the network corresponding to the $3_1\#3_1$ knot start both to grow proportional to N. This can be interpreted by assuming that the two knots are both localized at different, arbitrary positions along the ring. The

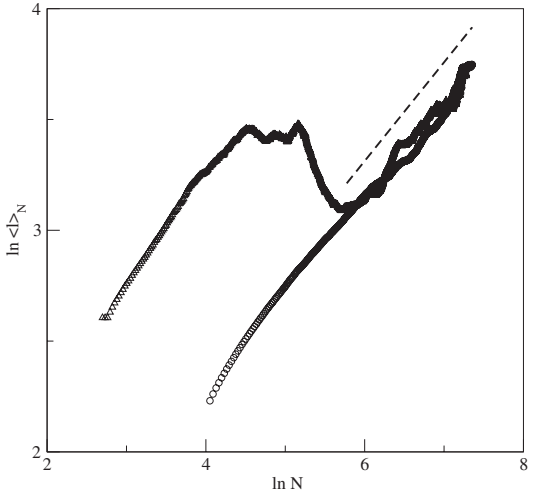

Fig. 6. Log-log plot of the average length of the third largest arc as a function of N for a ring with the topology of the $3_1\#3_1$ (top). For comparison we show a similar plot for the length of the second largest arc for the trefoil. The data are for $T = T_\theta$. The dashed line has slope 0.44.

two largest segments with average length $\propto N$ are simply the complementary arcs into which the centers of the knots partition the whole ring. On the other hand, the third longest segment appears to grow asymptotically as a power of N which is very close to the one appropriate for $\langle l_5 \rangle_N$ in the case of a single 3_1 knot. All this is well illustrated in Fig. 6 where the plot of $\ln \langle l_{10} \rangle_N$ for the $3_1\#3_1$ knot is reported together with that of $\langle l_5 \rangle_N$ in the 3_1 case. The plots are suitably shifted in such a way to overlap their most asymptotic portions. The drop observed for $\langle l_{10} \rangle_N$ between $\ln N \sim 4$ and $\ln N \sim 6$ is due to the fact that in this interval $\langle l_{11} \rangle_N$ increases its growth rate with N, reaching $\langle l_{11} \rangle_N \sim \langle l_{12} \rangle_N \sim N$. This increase inhibits initially the growth of $\langle l_{10} \rangle_N$ and even reduces it. We also observed that, within the explored range of N, $\langle l_9 \rangle_N$ for the composite knot does always grow very weakly compared to $\langle l_{10} \rangle_N$. All these findings can be interpreted in terms of the contracted network picture sketched in Fig. 7. There we have again a figure eight in which the largest loop has total length $N - l_{10}$, but is divided into two arcs by the 4-leg vertex and by another 2-leg vertex which represents the most localized component of the knot. This last component will be assumed to be pointlike compared to the other one, which in turn develops the smaller loop of the figure eight network.

The partition function describing such a network has the form

$$Z_C(N - l_{10}, l_{10}) \sim \int_a^{N-a} dx\, K_c^{-N} (N_{10})^{\gamma_8 - 1} F_C\left(\frac{x}{N_{10}}, \frac{l_{10}}{N_{10}}\right) \tag{6}$$

where we indicate by l_{10} the length of the smaller loop and $N_{10} = N - x - l_{10}$. In Eq. (6) C stands for the network of Fig. 7, and a represents a lower cut-off. Since $\sigma_2 = 0$ we have $\gamma_C = \gamma_8$. The two statistically longest segments are those of length x and $N - l_{10} - x$ and the integration in x takes into account the arbitraryness of the relative position of the two components. Consider now the limit $l_{10}/N \to 0$. It is clear that Eq. (6) in such

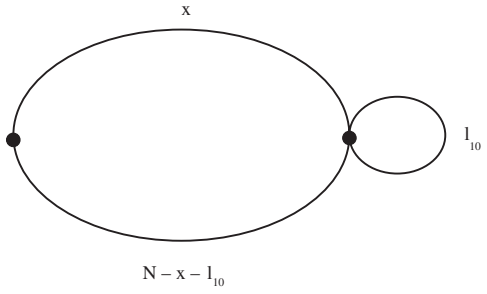

Fig. 7. Polymer network representing the composite knot $3_1\#3_1$ at the theta-temperature.

limit must reduce to the partition function of a ring with two 2-leg vertex insertions (a network which we denote by C_0), which is

$$Z_{C_0}(N) \sim \int_a^{N-a} dx\, K_c^{-N} (N-x)^{-3/2} F_{C_0}\left(\frac{x}{N-x}\right), \tag{7}$$

where we took into account that $\gamma_{C_0} = 1 - dv = -1/2$. Since this last partition must be simply $\sim NZ_o$, with Z_o given in Eq. (4), the scaling function F_{C_0} must reduce to a constant. This makes easy the matching of Eqs. (6) and (7) in the limit. Indeed, this simply leads to

$$F_G\left(\frac{x}{N-x-l_{10}}, \frac{l_{10}}{N-x-l_{10}}\right) \sim \left(\frac{l_{10}}{N-x-l_{10}}\right)^{-c}, \tag{8}$$

with c taking the same value as in the case of the prime 3_1 knot. So, the third longest arc in the $3_1\#3_1$ knot has a length probability distribution decaying with the same power as $p(l_5)$ for the 3_1 knot. This justifies the coincidence of asymptotic slopes displayed in Fig. 6.

For the $3_1\#3_1$ knot we did also obtain evidence that delocalization occurs at $T < T_\Theta$. Indeed, after a long transient, $\langle l_{10} \rangle_N$ starts eventually to grow more rapidly, in a way approximately compatible with a proportionality to N.

6. CONCLUSIONS

Our results show that the flat knots of an interacting ring polymer in two dimensions undergo a delocalization transition when the chain passes from the high-T swollen regime to the low-T compact one. At $T > T_\Theta$ both prime and composite knots are strongly localized, with size distributions having finite first moments as $N \to \infty$ ($t = 0$).[39, 51] On the other hand, below the theta point the average sizes of the knots diverge proportional to N. Right at $T = T_\Theta$, the knots are weakly localized, i.e., their average size grows as N^t with $t = 0.44 \pm 0.02$.

Configurations that have the shape of a figure eight dominate the statistics at the theta point, as was already found to be the case for flat knotted rings in a good solvent regime.[39, 51] This dominance allows to exploit results of the theory of polymer networks of fixed topology in order to conjecture $t = 3/7$ as the exact exponent characterizing the weak localization of flat knots at the theta point. Figure eight configurations are relevant also for temperatures below T_Θ, as demonstrated by our analysis of the preasymptotic behavior of $\langle l_5 \rangle_N$ for the 3_1 knot.

The scenario outlined above demonstrates a highly nontrivial interplay between topology and attractive interactions in a polymer system. Beyond the possible direct relevance of the model for applications, our results naturally suggest that qualitatively similar delocalization phenomena could be induced by the collapse transition also in the case of knotted polymers in three dimensions. A fundamental problem in that case is that of giving a meaningful definition of the size of a knot. In fact the present approach, which considers flat knots with minimal number of crossings, profits of the possibility of a simple and easily implementable definition of knot size. By allowing unrestricted crossings ($w = 1$), the problem of defining a flat knot size would present essentially the same difficulties as in three dimensions. However, some interesting proposals of such definition already exist.[43, 60] In the light of such definitions, knots of ring polymers in the good solvent regime are expected to be well localized.[33] This localization in good solvent is suggested also by studies in which the size of the knot is indirectly defined by making reference to the mechanical response of the polymer to an applied force.[44] If collapse induced delocalization could be demonstrated also for the three dimensional case, this phenomenon would have much impact in several contexts, ranging from protein folding, to the mechanical and dynamical properties of polymers.

ACKNOWLEDGMENTS

The work was supported by MIUR-COFIN01 and by INFM-PAIS02.

REFERENCES

1. S. Y. Shaw and J. C. Wang, Knotting of a DNA chain during ring closure, *Science* **260**:533–536 (1993).
2. V. L. Rybenkov, N. R. Cozzarelli, and A. Vologodskii, Probability of DNA knotting and the effective diameter of the DNA double helix, *Proc. Nat. Acad. Sci. USA* **90**:5307–11 (1993).
3. S. A. Wasserman and N. R. Cozzarelli, Biochemical topology: applications to DNA recombination and replication, *Science* **232**:951–960 (1986).
4. A. D. Bates and A. Maxwell, *DNA Topology* (IRL Press, 1993).
5. F. B. Dean, A. Stasiak, T. Koller, and N. R. Cozzarelli, Duplex DNA knots produced by Escherichia coli topoisomerase I, *J. Biol. Chem.* **260**:4795–4983 (1985).
6. C. D. Lima, J. C. Wang, and A. Mondragon, Three-dimensional structure of the 67K N-terminal fragment of E. coli DNA topoisomerase I, *Nature* **367**:138–146 (1994).
7. S. A. Wasserman and N. R. Cozzarelli, Supercoiled DNA-directed knotting by T4 topoisomerase, *J. Biol. Chem.* **266**, 20567–20573 (1991).

8. M. A. Krasnow, A. Stasiak, S. J. Spengler, F. Dean, T. Koller, and N. R. Cozzarelli, Determination of the absolute handedness of knots and catenanes of DNA, *Nature* **304**:559–560 (1983).
9. N. J. Crisona, *et al.*, Processive Recombination by Wild-Type Gin and an Enhancer-Independent Mutant: insight into the Mechanisms of Recombination Selectivity and Strand exchange, *J. Mol. Biol.* **243**:437–457 (1994).
10. S. A. Wasserman, J. M. Dungan, and N. R. Cozzarelli, Discovery of a predicted DNA knot substantiates a model for site-specific recombination, *Science* **229**:171–174 (1985).
11. A. Stasiak, V. Katritch, J. Bednar, D. Michoud, and J. Dubochet, Electrophoretic mobility of DNA knots, *Nature* **384**:122 (1996).
12. H. L. Frisch and E. Wasserman, Chemical Topology, *J. Am. Chem. Soc.* **83**:3789–3795 (1968).
13. M. Delbruck, *Mathematical Problems in the Biological Sciences* (AMS, Providence, RI, 1962), p. 55.
14. D. W. Sumners and S. G. Whittington, Knots in self-avoiding walks, *J. Phys. A: Math. Gen.* **21**:1689–1694 (1988).
15. N. Pippenger, Knots in random walks, *Disc. Appl. Math.* **25**:273–278 (1989).
16. K. Koniaris and M. Muthukumar, Knottedness in ring polymers, *Phys. Rev. Lett.* **66**:2211–2214 (1991).
17. P.-G. de Gennes, Tight knots, *Macromolecules* **17**:703–704 (1984).
18. T. Strick, J. F. Allemand, V. Croquette, and D. Bensimon, The manipulation of single biomolecules, *Physics Today* **54**:46–51 (2001).
19. S. F. Edwards, Statistical mechanics with topological constraints: I, *Proc. Phys. Soc.* **91**:513–519 (1967).
20. A. V. Vologodskii, A. V. Lukashin, M. D. Frank-Kamenetskii, and V. V. Anshelevich, The knot probability in statistical mechanics of polymer chains, *Sov. Phys. JETP* **39**:1059–1063 (1974).
21. M. D. Frank-Kamenetskii, A. V. Lukashin, and A. V. Vologodskii, Statistical mechanics and topology of polymer chains, *Nature* **258**:398–402 (1975).
22. J. P. J. Michels and F. W. Wiegel, On the topology of a polymer ring, *Proc. Roy. Soc. A* **403**:269–284 (1986).
23. S. F. Edwards, Statistical mechanics with topological constraints: II, *J. Phys. A* **1**:15–28 (1968).
24. T. Deguchi and K. Tsurusaki, Topology of closed random polygons, *J. Phys. Soc. Japan* **62**:1411–1414 (1993).
25. E. Orlandini, E. J. Janse van Rensburg, M. C. Tesi, D. W. Sumners, and S. G. Whittington, *Topology and Geometry of Biopolymers (IMA Volumes in Mathematics and its Applications)*, **82**:21–37 (1996).
26. A. Yu. Grosberg and S. Nechaev, Algebraic invariants of knots and disordered Potts model, *J. Phys. A* **25**:4659–4672 (1992).
27. A. Yu. Grosberg, Critical exponents for random knots, *Phys. Rev. Lett.* **85**:3858–3861 (2000).
28. A. Yu. Grosberg, *Self-avoiding knots*, preprint, `cond-mat/0207427` (2002).
29. E. J. Janse van Rensburg and S. G. Whittington, The knot probability in lattice polygons, *J. Phys. A* **23**:3573–3590 (1990).
30. E. J. Janse van Rensburg and S. G. Whittington, The dimensions of knotted polygons, *J. Phys. A* **24**:3935–3948 (1991).
31. E. Orlandini, M. C. Tesi, E. J. Janse van Rensburg, and S. G. Whittington, Asymptotics of knotted lattice polygons, *J. Phys. A* **31**:5953–5967 (1998).

32. S. R. Quake, Topological effects of knots in polymers, *Phys. Rev. Lett.* **73**:3317–3320 (1994).
33. E. Orlandini, M. C. Tesi, E. J. Janse van Rensburg, and S. G. Whittington, Entropic exponents of lattice polygons with specified knot type, *J. Phys. A* **29**:L299–L303 (1996).
34. B. Maier and J. O. Rädler, Conformation and Self-Diffusion of Single DNA Molecules Confined in Two Dimensions, *Phys. Rev. Lett.* **82**:1911–1914 (1999).
35. E. Ben-Naim, Z. A. Daya, P. Vorobieff, and R. E. Ecke, Knots and random walks in vibrated granular chains, *Phys. Rev. Lett.* **86**:1411–1416 (2001).
36. M. B. Hastings, Z. A. Daya, E. Ben-Naim, and R. E. Ecke, Entropic tightening of vibrated chains, *Phys. Rev. E* **66**:R25102–R25105 (2002).
37. K. Murasugi, *Knot theory and its applications* (Birkhäuser, Boston, 1996).
38. E. Guitter and E. Orlandini, Monte Carlo results for projected self-avoiding polygons: a two-dimensional model for knotted polymers, *J. Phys. A* **32**:1359–1385 (1999).
39. R. Metzler, A. Hanke, P. G. Dommersnes, Y. Kantor, and M. Kardar, Equilibrium shapes of flat knots, *Phys. Rev. Lett.* **88**:188101 (2002).
40. B. Duplantier, Statistical mechanics of polymer networks of any topology, *J. Stat. Phys.* **54**:581–680 (1989).
41. K. Ohno and K. Binder, Theory of star polymers and general polymer networks in bulk and semi-infinite good solvents, *J. Phys. (Paris)* **49**:1329–1352 (1988).
42. Y. Kafri, D. Mukamel, and L. Peliti, Why is the DNA denaturation transition first order?, *Phys. Rev. Lett.* **85**:4988–4991 (2000).
43. V. Katrich, W. K. Olson, A. Vologodskii, J. Dubochet, and A. Stasiak, Tightness of random knotting, *Phys. Rev. E* **61**:5545–5549 (2000).
44. O. Farago, Y. Kantor, and M. Kardar, Pulling knotted polymers, *Europhys. Lett.* **60**:53–59 (2002).
45. C. Vanderzande, *Lattice models of polymers* (Cambridge University Press, 1998).
46. F. Takusagawa and K. Kamitori, A real knot in protein, *Am. Chem. Soc.* **118**:8945–8946 (1996).
47. W. R. Taylor, A deeply knotted protein structure and how it might fold, *Nature* **406**:916–919 (2000).
48. V. S. Pande and D. S. Rokhsar, Is the molten globule a third phase of proteins?, *Proc. Natl. Acad. Sci. USA* **95**:1490–1494 (1998).
49. P. G. Dommersnes, Y. Kantor, and M. Kardar, Knots in charged polymers, *Phys. Rev. E* **66**:031802 (2002).
50. M. Baiesi, E. Carlon, and A. L. Stella, Scaling in DNA unzipping models: denaturated loops and end segments as branches of a block copolymer network, *Phys. Rev. E* **66**:021804 (2002).
51. E. Orlandini, A. L. Stella, and C. Vanderzande, The polymer theta-point as a knot delocalization transition, cond-mat/0211259 (2002); *Phys. Rev. E* **68**:031804 (2003).
52. B. Nienhuis, Exact critical point and critical exponents of $O(n)$ models in two dimensions, *Phys. Rev. Lett.* **49**:1062–1065 (1982).
53. M. C. Tesi, E. J. Janse van Rensburg, E. Orlandini, and S. G. Whittington, Monte Carlo study of the interacting self-avoiding walk model, *J. Stat. Phys.* **82**:155–181 (1996).
54. E. Orlandini, Monte Carlo study of polymer systems by multiple Markov Chain method, *IMA Proc. Work.* **102**:33–57 (1996).
55. B. Duplantier and H. Saleur, Exact tricritical exponents for polymers at the Θ-point in two dimensions, *Phys. Rev. Lett.* **59**:539–542 (1987).
56. F. Seno and A. L. Stella, θ point of a linear polymer in 2 dimensions: a renormalisation group analysis of Monte Carlo enumerations, *J. Phys.* **49**:739–748 (1988).

57. H.-P. Hsu and P. Grassberger, Collapsed 2-dimensional polymers on a cylinder, *J. Phys. A* **35**:L759–L766 (2002).
58. L. Schäfer, C. von Ferber, U. Lehr, and B. Duplantier, Renormalization of polymer networks and stars, *Nucl. Phys. B* **374**:473–495 (1992).
59. B. Duplantier and H. Saleur, Exact critical properties of two-dimensional dense self-avoiding walks, *Nucl. Phys. B* **290**:291–326 (1987).
60. E. J. Janse van Rensburg, D. W. Sumners, E. Wassermann, and S. G. Whittington, Entanglement complexity of self-avoiding walks, *J. Phys. A* **25**:6557–6566 (1992).